# The EXS Domain of PHO1 Participates in the Response of Shoots to Phosphate Deficiency via a Root-to-Shoot Signal[1][OPEN]

**Stefanie Wege[2], Ghazanfar Abbas Khan, Ji-Yul Jung, Evangelia Vogiatzaki, Sylvain Pradervand, Isabel Aller, Andreas J. Meyer, and Yves Poirier***

Department for Plant Molecular Biology (S.W., G.A.K., J.-Y.J., E.V., Y.P.) and Genomic Technologies Facility, Center for Integrative Genomics (S.P.), University of Lausanne, 1015 Lausanne, Switzerland; Vital-IT, Swiss Institute of Bioinformatics, 1015 Lausanne, Switzerland (S.P.); and Institute for Crop Science and Natural Resources, Chemical Signaling, University of Bonn, 53113 Bonn, Germany (I.A., A.J.M.)

**ORCID IDs: 0000-0002-7232-5889 (S.W.); 0000-0002-7557-6210 (G.A.K.); 0000-0003-2503-316X (E.V.); 0000-0002-0501-807X (I.A.); 0000-0001-8144-4364 (A.J.M.); 0000-0001-8660-294X (Y.P.).**

The response of shoots to phosphate (Pi) deficiency implicates long-distance communication between roots and shoots, but the participating components are poorly understood. We have studied the topology of the Arabidopsis (*Arabidopsis thaliana*) PHOSPHATE1 (PHO1) Pi exporter and defined the functions of its different domains in Pi homeostasis and signaling. The results indicate that the amino and carboxyl termini of PHO1 are both oriented toward the cytosol and that the protein spans the membrane twice in the EXS domain, resulting in a total of six transmembrane $\alpha$-helices. Using transient expression in *Nicotiana benthamiana* leaf, we demonstrated that the EXS domain of PHO1 is essential for Pi export activity and proper localization to the Golgi and trans-Golgi network, although the EXS domain by itself cannot mediate Pi export. In contrast, removal of the amino-terminal hydrophilic SPX domain does not affect the Pi export capacity of the truncated PHO1 in *N. benthamiana*. While the Arabidopsis *pho1* mutant has low shoot Pi and shows all the hallmarks associated with Pi deficiency, including poor shoot growth and overexpression of numerous Pi deficiency-responsive genes, expression of only the EXS domain of PHO1 in the roots of the *pho1* mutant results in a remarkable improvement of shoot growth despite low shoot Pi. Transcriptomic analysis of *pho1* expressing the EXS domain indicates an attenuation of the Pi signaling cascade and the up-regulation of genes involved in cell wall synthesis and the synthesis or response to several phytohormones in leaves as well as an altered expression of genes responsive to abscisic acid in roots.

Phosphate (Pi) homeostasis in complex multicellular organisms is dependent on a range of transporters involved in both Pi import into cells as well as Pi export to the extracellular space. In roots, Pi export to the apoplast in the stele is essential for the transfer of Pi from roots to shoots via xylem vessels (Poirier and Bucher, 2002). Pi export is also essential for the transfer of Pi from the mycorrhizal arbuscules to the root cells (Bonfante and Genre, 2010) and to tissues that are not symplastically connected to their neighbors, such as the developing embryos and pollen grains (Stadler et al., 2005).

Arabidopsis (*Arabidopsis thaliana*) PHOSPHATE1 (PHO1) is the prototypical eukaryotic Pi exporter. PHO1 is primarily expressed in the root stelar cells, where it acts to load Pi into the xylem apoplastic space (Poirier et al., 1991; Hamburger et al., 2002). Arabidopsis and rice (*Oryza sativa*) *pho1* mutants are defective in the transfer of Pi from roots to shoots, leading to Pi-deficient shoots (Poirier et al., 1991; Secco et al., 2010). Expression of PHO1 in heterologous plant tissues, such as leaf mesophyll cells, leads to specific Pi export to the apoplast (Arpat et al., 2012). Surprisingly, PHO1 is localized to the Golgi and the trans-Golgi network (TGN), raising interesting questions regarding how PHO1 could mediate Pi export (Arpat et al., 2012; Liu et al., 2012). It is possible that Pi export is mediated by a small fraction of PHO1 protein localized to the plasma

[1] This work was supported by the Swiss National Foundation (grant nos. 31003A–138339 and 31003A–159998), the Marie Curie Intra-European Fellowship PHOSTASIA (grant no. 298843), and the Deutsch Forschungsgemeinschaft (Major Research Instrumentation grant no. INST 217/651–1 FUGG).

[2] Present address: Australian Research Council Centre of Excellence in Plant Energy Biology, School of Agriculture, Food, and Wine, Waite Research Institute, University of Adelaide, Glen Osmond, South Australia 5064, Australia.

* Address correspondence to yves.poirier@unil.ch.

The author responsible for distribution of materials integral to the findings presented in this article in accordance with the policy described in the Instructions for Authors (www.plantphysiol.org) is: Yves Poirier (yves.poirier@unil.ch).

S.W. and Y.P. designed experiments, analyzed transcriptome data, and wrote the article; S.W. performed all experiments, except G.A.K. performed Q-RT-PCR, J.-Y.J. performed western-blot analysis, S.P. performed analysis of the RNAseq data, and S.W. and E.V. performed grafting; I.A. and A.J.M. provided technical and analytical support for roGFP2 measurements.

[OPEN] Articles can be viewed without a subscription.
www.plantphysiol.org/cgi/doi/10.1104/pp.15.00975

  

membrane, as for the IRT1 iron transporter (Barberon et al., 2011). Alternatively, PHO1 could mediate Pi export through the loading of Pi into endosomes, followed by the release of Pi to the extracellular space via exocytosis (Arpat et al., 2012). The *pho1* null mutants have small rosettes and show the hallmarks of Pi deficiency, including anthocyanin accumulation and the overexpression of a number of genes associated with Pi deficiency. In contrast, knockdown of *PHO1* via gene silencing led to plants that had reduced shoot Pi content but maintained normal shoot growth and had an attenuated transcriptional response to Pi deficiency (Rouached et al., 2011). These results indicated a role for PHO1 in mediating the response of plants to Pi deficiency.

PHO1 homologs are present in all land plants, including lycophytes, bryophytes, and gymnosperms (Wang et al., 2008; He et al., 2013). PHO1 homologs are also present in fungi and animals, including mammals. The mammalian PHO1 homolog, named XPR1, was initially identified as a protein acting as a cell surface receptor for retroviruses (Battini et al., 1999; Yang et al., 1999). Heterologous expression of XPR1 either in *Nicotiana benthamiana* or in mammalian cultured cells showed that it also acts as a Pi exporter (Giovannini et al., 2013; Wege and Poirier, 2014). PHO1 proteins are composed of three distinct regions (Wang et al., 2004). The N-terminal half of the protein is hydrophilic and composed of a tripartite SPX domain. SPX domains are found in a variety of evolutionarily unrelated proteins implicated in Pi metabolism (Secco et al., 2012). In fungi, SPX-containing proteins include PHO81 and PHO87, acting in Pi sensing and transport, and VTC4, involved in polyphosphate synthesis (Wykoff and O'Shea, 2001; Hothorn et al., 2009). In addition to PHO1, plants have a number of SPX-containing proteins, including NLA1, a protein involved in ubiquitination of the PHT1 Pi transporter (Kant et al., 2011; Lin et al., 2013), and the SPX1, SPX2, and SPX4 proteins that bind to and modulate the activity of PHR1, the primary transcription factor mediating the response to Pi deficiency in plants (Lv et al., 2014; Puga et al., 2014; Wang et al., 2014). Following the SPX domain, PHO1 has a series of putative transmembrane $\alpha$-helices that are partly included in the C-terminal EXS domain. EXS is named for a homologous region found in the two yeast (*Saccharomyces cerevisiae*) proteins ERD1 and SYG1 and the mammalian XPR1 (Wang et al., 2004). No function has yet been assigned to the EXS domain.

In this work, the topology of Arabidopsis PHO1 was first studied using the techniques of bimolecular fluorescence complementation (BiFC) and redox-sensitive GFP (roGFP2) as reporters for membrane protein orientation. The role of each PHO1 domain in the localization and activity of PHO1 was studied through the expression of various combinations of PHO1 domains, both transiently in *N. benthamiana* and stably in transgenic *pho1* mutants. The results show that the EXS domain is crucial for the localization and Pi export activity of PHO1. Furthermore, expression of only the EXS domain in roots of the *pho1* mutant resulted in the stimulation of shoot growth and the attenuation of the Pi deficiency signaling cascade, revealing an important role for the EXS domain in modulating the Pi deficiency response via a long-distance root-to-shoot signal.

## RESULTS

### Topology of PHO1

Analysis of PHO1 using algorithms available online on TOPCONS (http://topcons.cbr.su.se/; Bernsel et al., 2009) and ARAMEMNON (http://aramemnon.botanik.uni-koeln.de/; Schwacke et al., 2003) revealed numerous potential transmembrane-spanning $\alpha$-helices in the C-terminal half of the protein (Fig. 1). While there is broad agreement between all prediction programs for the localization of the first four transmembrane $\alpha$-helices, predictions for the number and position of further transmembrane $\alpha$-helices in the EXS domain of PHO1 are highly variable, ranging between zero and six. This leads to uncertainties regarding whether the C-terminal end of PHO1 is on the same or the opposite side compared with the N terminus (Fig. 1; Supplemental Fig. S1). In our analysis, PHO1 has thus been partitioned into three main regions, namely the hydrophilic region containing the SPX domain, the hydrophobic region harboring the first four transmembrane $\alpha$-helices (4TM), and the following hydrophobic region harboring the EXS domain (Fig. 1A). We concentrated our effort to study the topology of the EXS domain, while investigation of the N-terminal domain was limited to determining whether the hydrophilic SPX domain was in the cytosol or the Golgi/TGN lumen.

For localization of the SPX domain, we used a method based on BiFC in transiently transformed *N. benthamiana* leaves that is adapted for membrane proteins located in the endoplasmic reticulum (ER)/Golgi (Zamyatnin et al., 2006; Sparkes et al., 2010). This method is based on the targeted expression, using a strong cauliflower mosaic virus 35S promoter, of a free half of the yellow fluorescent protein (YFP) that is either localized in the cytosol and nucleus or directed into the lumen of the ER via a specific recognition sequence. The other half of YFP is then fused to the protein of interest, and reconstitution of YFP fluorescence is possible only if the two YFP halves are expressed on the same side of the membrane (i.e. the cytosolic or luminal side of the ER/Golgi). The C-terminal half of the yellow fluorescent protein (YC) was fused to the N terminus of full-length PHO1 (YC-PHO1) or a truncated version without the SPX domain but containing all potential transmembrane $\alpha$-helices (YC-4TMEXS; see purple stars in Fig. 1). For both constructs, we could observe a punctate fluorescent signal when coexpressed with a cytosolic N-terminal half of YFP (YN-cyto), but no punctate fluorescence was observed when coexpressed with an N-terminal half of YFP localized in the ER/Golgi lumen (YN-lumen; Fig. 2; Supplemental Fig. S2).

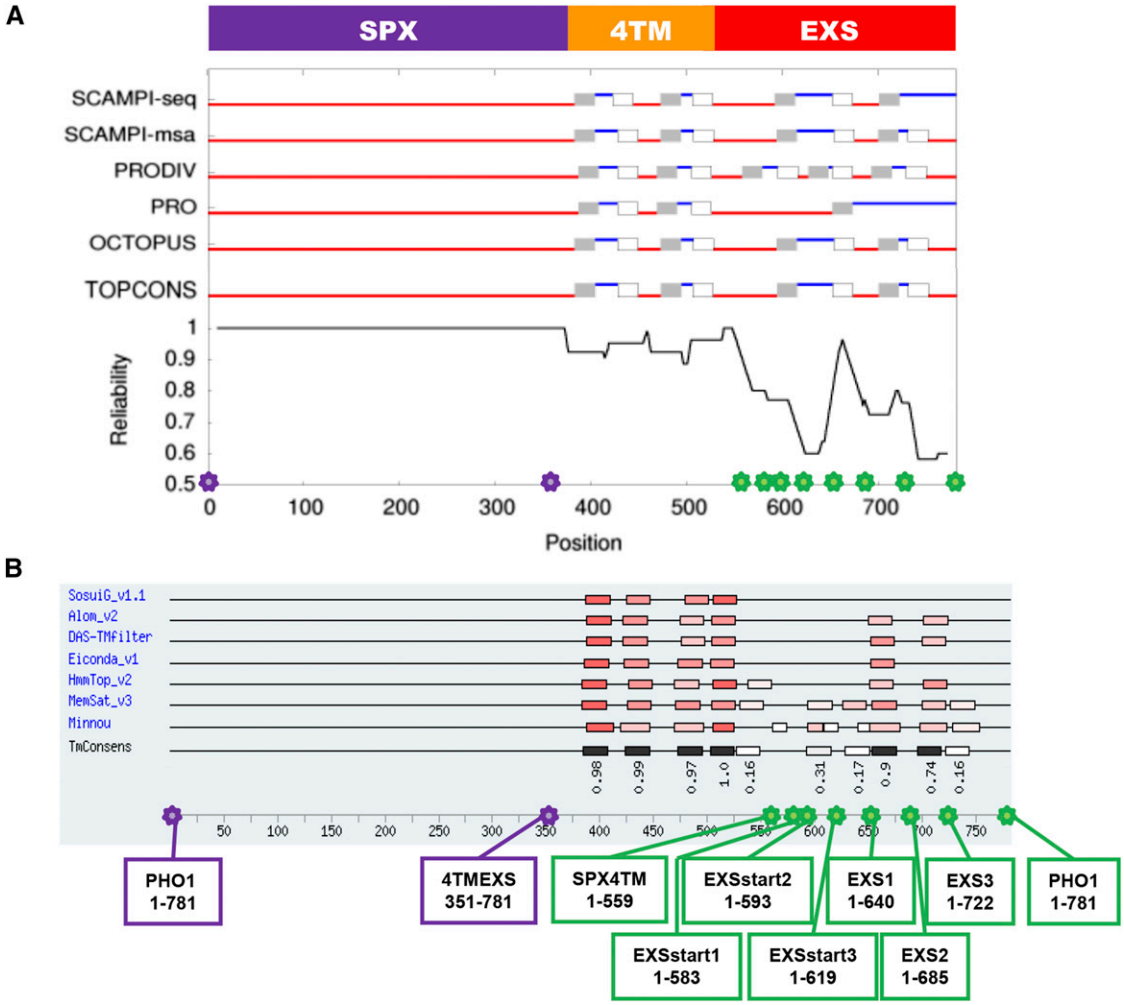


**Figure 1.** Topology of the PHO1 protein. A, Predicted topologies according to TOPCONS (http://topcons.cbr.su.se/). Red and blue lines indicate inside and outside, respectively, while boxes indicate transmembrane regions. B, Selected predicted topologies according to ARAMEMNON (http://aramemnon.botanik.uni-koeln.de/). The intensity of the red color in boxes reflects the level of hydrophobicity of the putative transmembrane domains predicted by each program. Similarly, the intensity of the black color reflects the score value for a transmembrane domain in the consensus prediction. For complete predictions according to ARAMEMNON, see Supplemental Figure S1. Positions of N- and C-terminal truncations are indicated as purple and green stars, respectively, and the corresponding names of the truncations and amino acids are indicated in boxes below each star in B.

The punctate pattern observed in the coexpression with YN-cyto is in agreement with the localization of PHO1 in the Golgi/TGN (Arpat et al., 2012). Constructs encoding for the cytosolic or luminal ER/Golgi YN and YC are well expressed and give a strong fluorescent signal when expressed in the same compartment, confirming that they reassemble correctly in our experimental conditions (Fig. 2; Supplemental Fig. S2). These results show that the SPX domain of PHO1 is localized in the cytosol and that the first transmembrane-spanning $\alpha$-helix enters the membrane from the cytosolic side.

To determine the topology of the EXS domain, we used a method relying on a redox-sensitive GFP named roGFP2 (Brach et al., 2009). This method is based on the different redox potentials of the cytosol and the lumen of the ER and Golgi, leading to a predominantly reduced form of roGFP2 in the cytosol and an oxidized form in the ER/Golgi lumen. These two states of roGFP2 have different excitation properties enabling ratiometric measurements. The ratios of emission generated by excitation at 405 and 488 nm, respectively, define if the roGFP2 is localized in the ER/Golgi lumen or in the cytosol (Brach et al., 2009). This technique was successfully used to determine the topology of Arabidopsis membrane proteins in *N. benthamiana* cells such as the K/HDEL receptor ERD2 (Brach et al., 2009), the ER-associated proteins KMS1 and KMS2 (Wang et al., 2011), a splice variant of YUCCA4 involved in auxin biosynthesis (Kriechbaumer et al., 2012), and five distinct reticulons (Sparkes et al., 2010). roGFP2 was fused to the C terminus of full-length PHO1 and of different

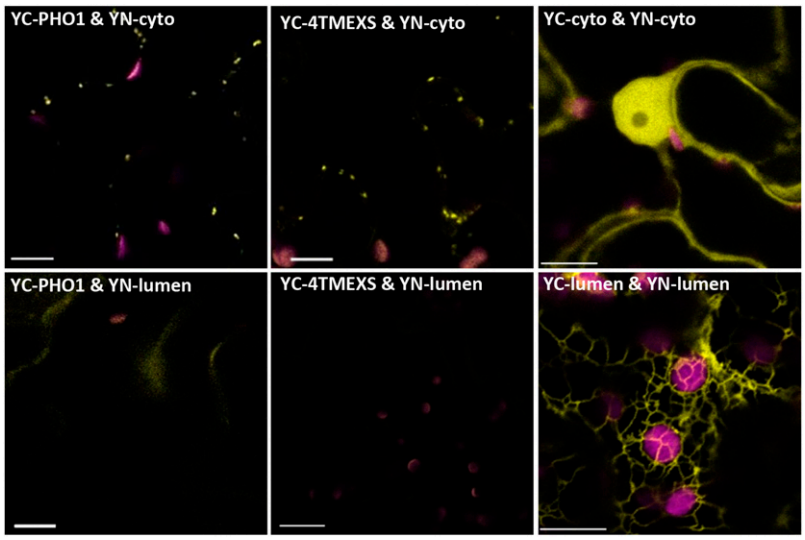


**Figure 2.** Investigation of PHO1 topology using BiFC in *N. benthamiana*. Confocal images show BiFC YFP signal in yellow and chloroplast chlorophyll autofluorescence in magenta. The C-terminal half of YFP was fused to the N terminus of either full-length PHO1 (YC-PHO1; left column) or the 4TMEXS truncation (YC-4TMEXS; middle column) and coexpressed with either the free N-terminal half of YFP expressed in the cytosol (YN-cyto; top row) or the ER/Golgi lumen (YN-lumen; bottom row). BiFC signal is obtained when either YC-PHO1 or YC-4TMEXS is coexpressed with YN-cyto but not with YN-lumen. As controls, cytosolic and nuclear BiFC signal is obtained when YN-cyto is coexpressed with YC-cyto (top right) and an ER BiFC signal is obtained when YN-lumen and YC-lumen are coexpressed in the ER lumen (bottom right). Bars = 10 $\mu$m.

C-terminal truncations of PHO1, and all constructs were transiently expressed in *N. benthamiana*. The truncations were placed between potential transmembrane segments according to the topology predictions of TOPCONS and ARAMEMNON. The truncations are named according to their new C termini (see also green stars in Fig. 1): SPX4TM (amino acids 1–559-roGFP2), EXSstart1 (amino acids 1–583-roGFP2), EXSstart2 (amino acids 1–593-roGFP2), EXSstart3 (amino acids 1–619-roGFP2), EXS1 (amino acids 1–640-roGFP2), EXS2 (amino acids 1–685-roGFP2), and EXS3 (amino acids 1–722-roGFP2) as well as full-length PHO1 (amino acids 1–781-roGFP2; Fig. 1, green stars). The fusion proteins were transiently expressed in *N. benthamiana* leaves via *Agrobacterium tumefaciens* infiltration. The 405:488 ratios obtained with leaf pieces incubated in water were compared with the control ratios obtained with pieces of the same leaf incubated in a solution containing either hydrogen peroxide (H2O2) or dithiothreitol (DTT) to obtain fully oxidized or reduced roGFP2, respectively. Two exemplary false-color image sets for the truncated PHO1-roGFP2 fusions, EXSstart2 and EXSstart3, where the C-terminal roGFP2 is oriented to the cytosol and the ER/Golgi lumen, respectively, are shown in Figure 3A. The full set of measurements obtained for all constructs is shown in Figure 3B. The results show that the C terminus of full-length PHO1 is localized toward the cytosol as well as the C termini of the truncations SPXTM4, EXSstart1, EXSstart2, EXS1, EXS2, and EXS3, while only the C terminus of truncation EXSstart3 is localized toward the lumen. Together, these results obtained with BiFC and roGFP2 reveal that the N and C termini of PHO1 are both oriented toward the cytosol and suggest that the protein spans the membrane twice in the EXS domain, resulting in a total of six transmembrane $\alpha$-helices (Fig. 3C).

### Distinct Domains of PHO1 Are Responsible for Subcellular Localization and Pi Export

In order to study the contribution of the PHO1 domains to its subcellular localization, various truncations of PHO1 were fused to GFP or red fluorescent protein (RFP). Transient expression of fusion proteins in *N. benthamiana* leaves was used as the preferred experimental system, since colocalization of PHO1-GFP with subcellular markers in Arabidopsis roots has proven to be inadequate due to the combination of poor resolution and weak expression of fluorescent marker proteins in root xylem parenchyma cells (Arpat et al., 2012). Furthermore, expression of either the Arabidopsis PHO1 or its human homolog XPR1 in *N. benthamiana* has previously been shown to mediate specific Pi export, revealing that *N. benthamiana* leaf is an appropriate tissue in which to assess PHO1 Pi export activity (Arpat et al., 2012; Wege and Poirier, 2014).

We first verified that a full-length PHO1-RFP fusion is localized to the same organelles as the previously studied PHO1-GFP fusion (i.e. in the Golgi and TGN; Arpat et al., 2012; Fig. 4A). Afterward, we investigated the localization of four different truncations of PHO1. We found that signals of two truncations, 4TMEXS-GFP (amino acids 351–781) and EXS-RFP (amino acids 593–781), colocalize with full-length PHO1-GFP or PHO1-RFP signal and, therefore, are localized in the Golgi and TGN (Fig. 4, B and C). This result indicates that neither the SPX domain nor the first four transmembrane helices are required for Golgi and TGN targeting. A GFP fusion construct composed of the SPX and 4TM regions (amino acids 1–592, SPX4TM-GFP or GFP-SPX4TM) but lacking the C-terminal EXS domain did not colocalize with PHO1-RFP (Fig. 4D) but rather with the ER marker ER-rk-mCherry (Fig. 4E; Nelson et al., 2007). Together, these results show that the EXS domain is necessary for PHO1 localization to the Golgi and TGN.

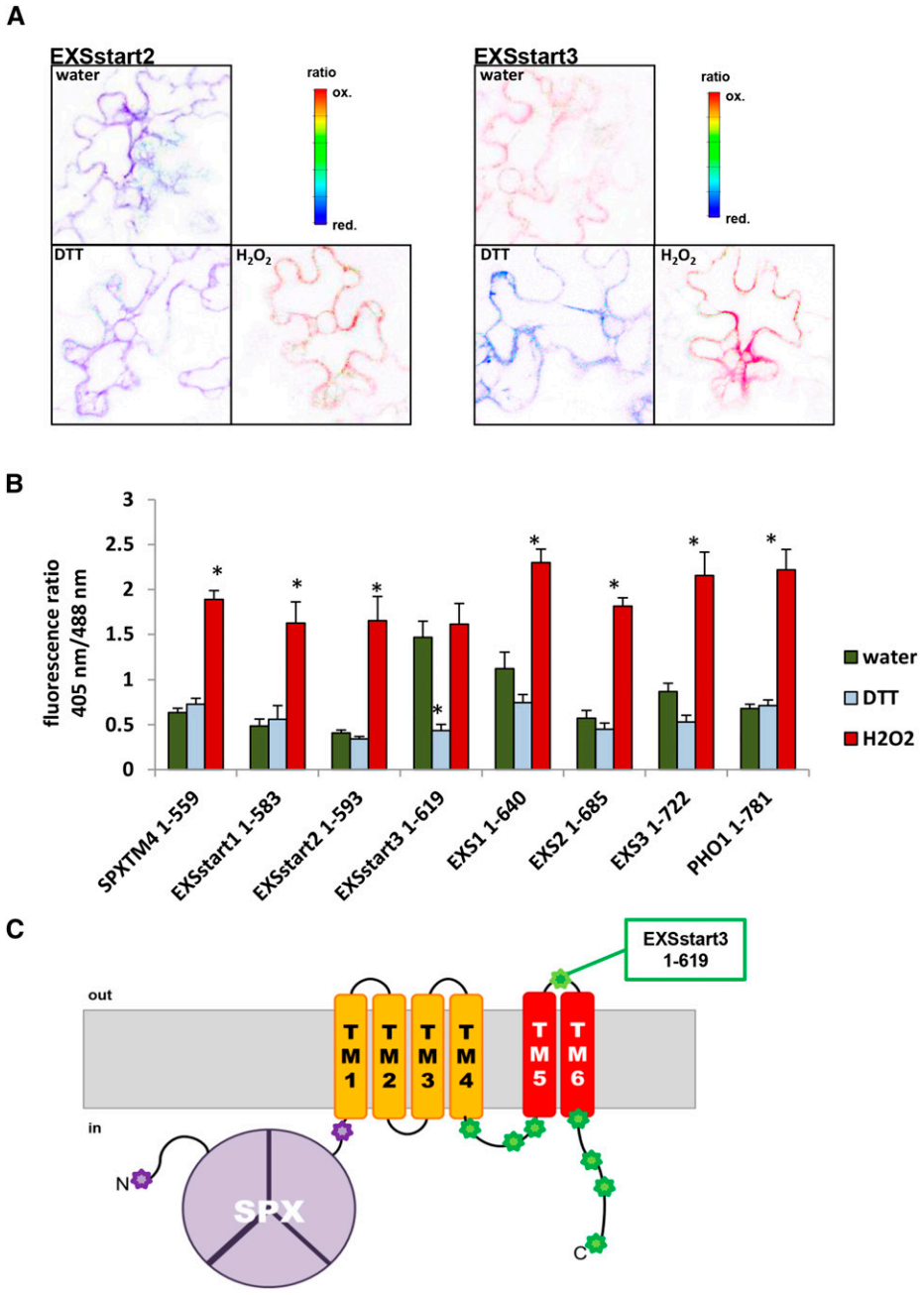


**Figure 3.** Investigation of the topology of the PHO1 EXS domain using roGFP2 in *N. benthamiana*. roGFP2 was fused to the C terminus of either full-length PHO1 or different PHO1 truncations. A, Example of two false-color image sets for the constructs EXSstart2-roGFP2 and EXSstart3-roGFP2 expressed transiently in leaf of *N. benthamiana* treated with water, DTT, or $H_2O_2$. B, Ratios for all PHO1-roGFP2 constructs (green) are compared separately with their respective DTT (blue) and $H_2O_2$ (red) controls. Error bars represent SD ($n$ = 11–32). Asterisks represent statistically significant differences compared with the corresponding water control (ANOVA, $P < 0.01$). C, Model of PHO1 topology according to BiFC and roGFP2 data with both termini localized in the cytosol and a total of six transmembrane-spanning segments. The SPX domain is displayed in purple, 4TM in orange, the transmembrane part of the EXS domain in red, N-terminal truncations as purple stars, C-terminal truncations as green stars, and the lumen-localized truncation EXSstart3 in the box.

Expression of only the SPX domain (amino acids 1–350, SPX-GFP or GFP-SPX) did not colocalize with PHO1-GFP (Fig. 5A) but was found in the nucleus, with a partially diffused nuclear signal and an apparent association with nuclear pores (Fig. 5B). To exclude the possibility that the nuclear localization of the SPX domain (estimated size of SPX-GFP was approximately 57 kD) was simply the result of diffusion, we expressed a triple GFP-tagged SPX (SPX-3xGFP) and confirmed its localization to the nucleus (Fig. 5, C and D). With a mass of approximately 120 kD, SPX-3xGFP is significantly larger than the size-exclusion limit of 40 kD for passive diffusion of proteins into the nucleus (Suntharalingam and Wente, 2003).

We next tested the capacity of the various truncated versions of PHO1 transiently expressed in *N. benthamiana* to mediate Pi export. Only expression of the 4TMEXS-GFP protein, composed of the full transmembrane part, led to specific Pi export at a level comparable to full-length PHO1-GFP (Fig. 6). Expression of all other truncations, including EXS-GFP, which has the same subcellular localization as full-length PHO1-GFP, did not lead to Pi export (Fig. 6).

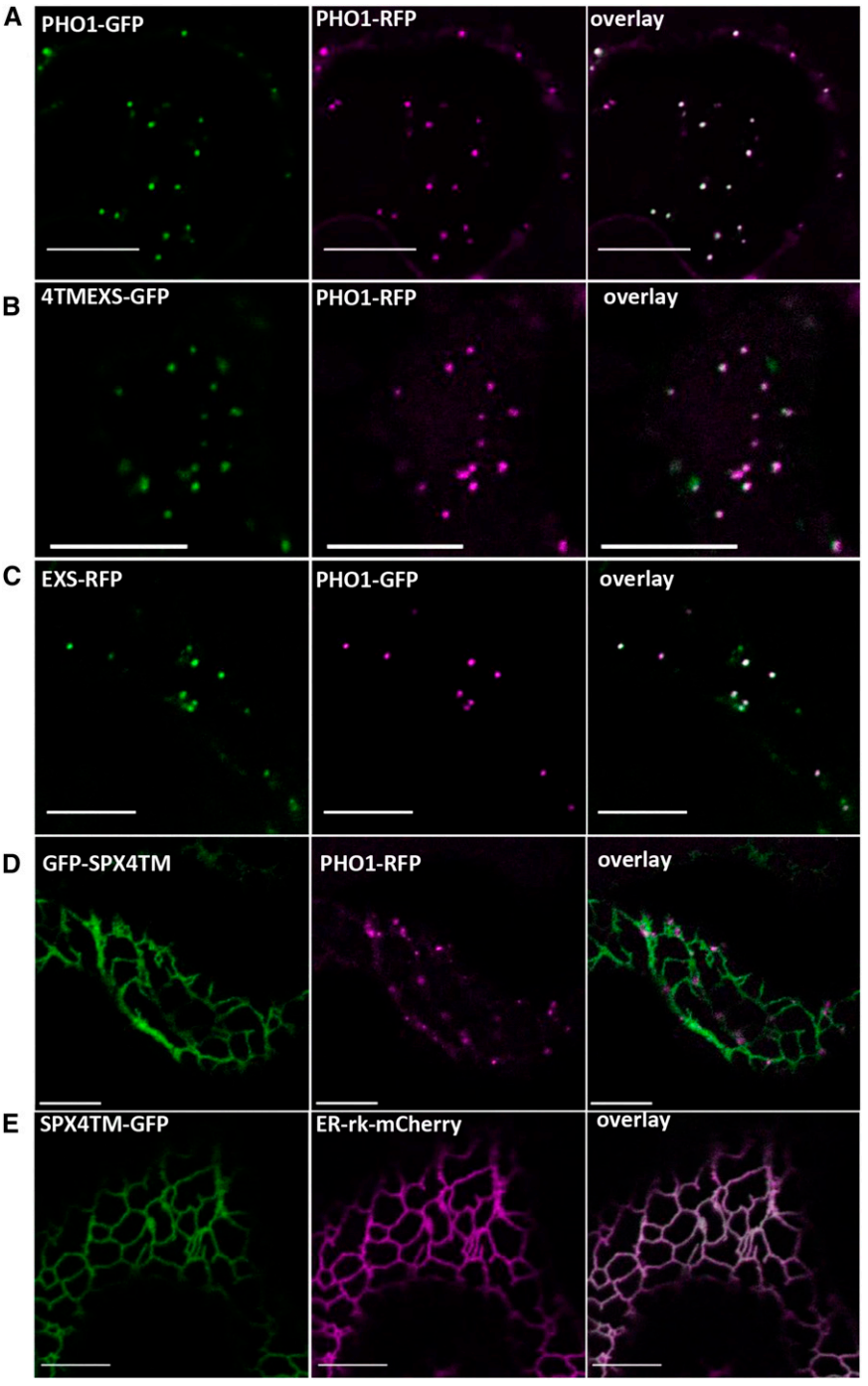


**Figure 4.** Subcellular localization of full-length and truncated PHO1 constructs transiently expressed in *N. benthamiana* epidermal cells. Fluorescent protein signal is shown in green in the left column, in magenta in the middle column, and signal overlay in white in the right column. A, Colocalization of PHO1-GFP (green) and PHO1-RFP (magenta) to the Golgi/TGN. B, Colocalization of 4TMEXS-GFP (green) and PHO1-RFP (magenta) to the Golgi/TGN. C, Colocalization of EXS-RFP (green) and PHO1-GFP (magenta) to the Golgi/TGN. D, Absence of colocalization of the ER GFP-SPX4TM (green) and Golgi/TGN PHO1-RFP (magenta). E, Colocalization of SPX4TM-GFP (green) and the ER-marker ER-rk-mCherry (magenta) to the ER. Bars = 10 $\mu$m.

### Expression of EXS in Roots of *pho1* Is Sufficient to Complement Shoot Growth But Not Pi Content

The Arabidopsis *pho1* mutant was stably transformed with all truncation constructs C-terminally tagged with GFP and expressed under the control of the *PHO1* promoter, enabling expression into the root vascular cylinder (Hamburger et al., 2002; Arpat et al., 2012; Liu et al., 2012). We previously showed that the expression of full-length *PHO1-GFP* complemented the *pho1* phenotype and led to wild-type shoot growth, seed yield, and shoot Pi content (Arpat et al., 2012). We first verified the subcellular localization of the fusion proteins in the root vascular cylinder. PHO1-GFP gave a punctate pattern expected for Golgi/TGN localization (Arpat et al., 2012; Fig. 7A). SPX-GFP gave a diffuse signal in the nucleus, and no association with the nuclear pores could be detected (Fig. 7B). 4TMEXS-GFP and EXS-GFP were both localized to punctate

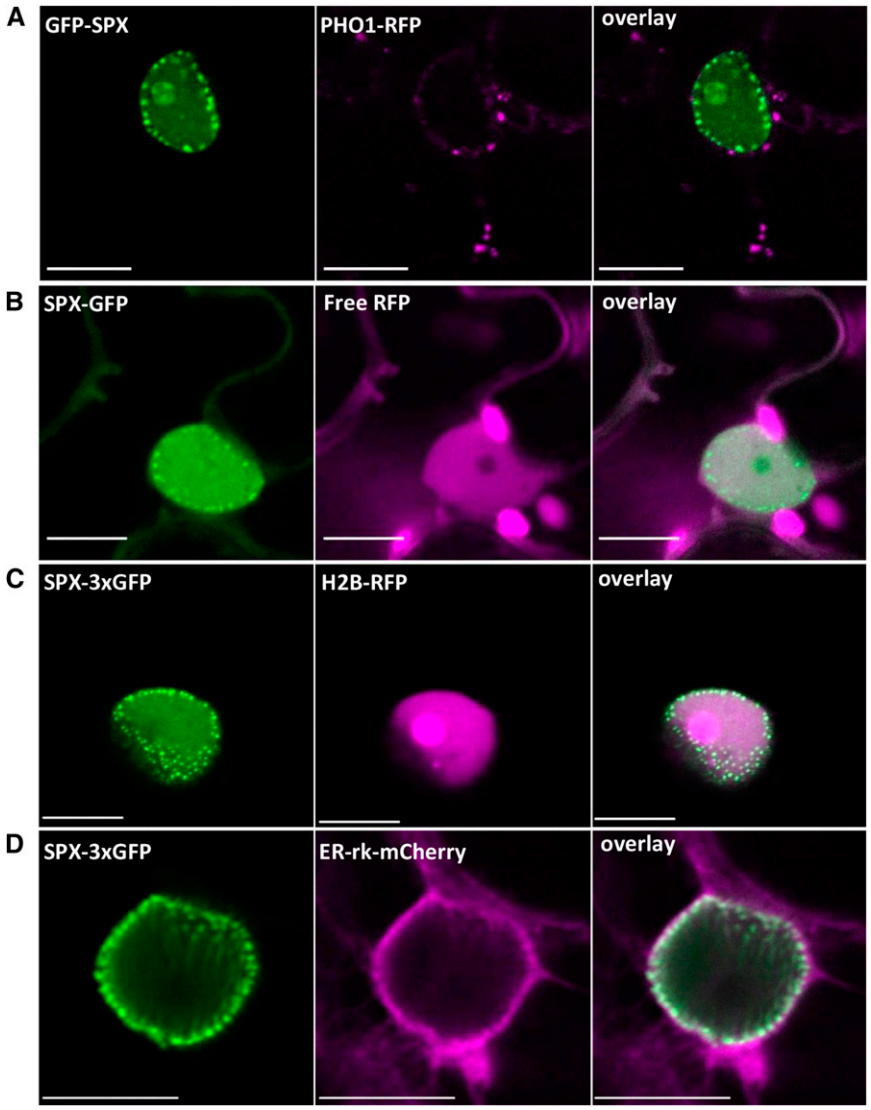


**Figure 5.** Subcellular localization of the SPX domain of PHO1 transiently expressed in *N. benthamiana* epidermal cells. GFP signal is shown in green in the left column, RFP or mCherry signal in magenta in the middle column, and signal overlay in white in the right column. A, Coexpression of GFP-SPX with the full-length PHO1-RFP. B, Coexpression of SPX-GFP and free RFP. Chloroplast chlorophyll autofluorescence appears as the strongest magenta signal. C, Coexpression of SPX-3xGFP and the nuclear marker H2B-RFP. D, Coexpression of SPX-3xGFP and the ER-marker ER-rk-mCherry. Bars = 10 $\mu$m.

structures similar to full-length PHO1-GFP, again likely representing Golgi/TGN (Fig. 7, C and D). Lines expressing EXS-GFP showed an additional weak fluorescent signal in the vacuole, possibly due to degradation (Fig. 7D). No stably transformed Arabidopsis line expressing SPX4TM-GFP could be obtained, although transient expression experiments showed that this protein was stable in *N. benthamiana* cells (Fig. 4D).

Expression of the various truncated PHO1-GFP constructs in the *pho1* background led to strikingly different phenotypes (Fig. 7E). Expression of 4TMEXS-GFP was deleterious to plant growth, giving plants that were much smaller than *pho1*, while the shoot Pi content was intermediate between *pho1* and wild-type plants (Fig. 7, E–G). Plants expressing SPX-GFP were comparable to *pho1* for both shoot fresh weight and Pi content (Fig. 7, E–G). Expression of EXS-GFP in the *pho1* background led to a remarkable improvement of shoot growth despite the maintenance of low shoot Pi comparable to *pho1* (Fig. 7, E–G). The phenotypes of these plants were comparable to the previously described transgenic lines B1 and B3 that underexpress *PHO1* via gene silencing, leading to reduced Pi transfer from roots to shoots, low shoot Pi, but the maintenance of wild-type-like shoot growth (Rouached et al., 2011). Thus, the expression of EXS-GFP in a *pho1* null mutant background led to an uncoupling of shoot Pi deficiency from its major effect on growth.

The *pho1-4* mutant allele used in this study has a point mutation at the 5′ splice junction of the 12th intron, abolishing splicing of this intron (Hamburger et al., 2002). If translated, such a mutated mRNA would produce a protein smaller than 17 kD and missing the last transmembrane domain in the EXS domain, which could potentially associate with an EXS-GFP protein, leading to intermolecular complementation. However, western-blot analysis of roots of the *pho1-4* mutant and lines EXS32 and EXS34 expressing EXS-GFP did not

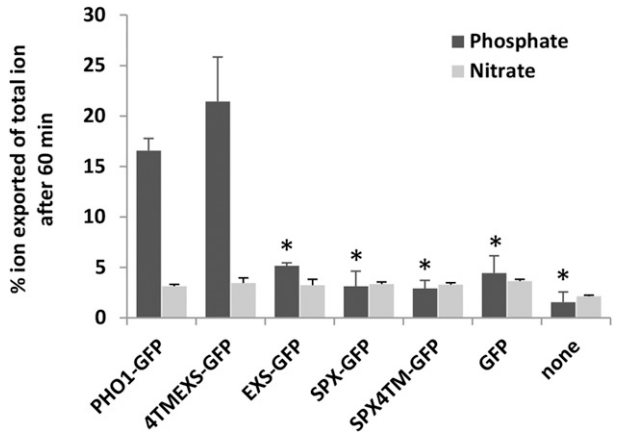


**Figure 6.** Measurement of Pi and nitrate export mediated by PHO1 and PHO1 truncations. PHO1 constructs were transiently expressed in *N. benthamiana* leaf discs, and the amount of Pi and nitrate exported to the apoplast was measured. As controls, Pi and nitrate export was measured in leaf discs expressing either GFP or not infiltrated (none). Errors bars represent SD ($n = 12$). Asterisks represent statistically significant differences compared with the PHO1-GFP control for each ion tested (ANOVA, $P < 0.01$).

reveal a detectable level of a truncated PHO1 protein in these lines (Fig. 7H), making intermolecular complementation unlikely.

While the *PHO1* promoter is predominantly active in the root vascular cylinder, *PHO1* expression is also expressed in shoots and guard cells (Hamburger et al., 2002; Zimmerli et al., 2012). Grafting experiments were thus performed to determine whether EXS-GFP expression in roots or shoots is responsible for the growth improvement of the *pho1* mutant. Shoots of Col-0 and *pho1* grafted onto roots of *pho1* expressing EXS-GFP developed rosettes that were comparable in size to the self-grafted Col-0 or self-grafted EXS-GFP plants while retaining a low shoot Pi comparable to the *pho1* mutant (Fig. 8). In contrast, shoots of *pho1* plants expressing EXS-GFP grafted onto roots of *pho1* developed rosettes that were comparable to self-grafted *pho1* and also contained low shoot Pi (Fig. 8). These results demonstrate that the expression of EXS-GFP in roots of *pho1* is sufficient to uncouple the reduction in shoot growth from low shoot Pi.

### Effect of the Expression of PHO1 Domains on the Pi Deficiency Transcriptome

To gain an in-depth analysis of the effects of EXS-GFP on the plant transcriptome, the expression profiles of roots and shoots of *pho1* complemented with a full-length PHO1-GFP construct (PHO1-C) and two independent *pho1* lines expressing EXS-GFP were compared with the *pho1* mutant using RNA sequencing (RNAseq). While the EXS32 and EXS34 lines showed overall similar shoot phenotype and shoot Pi content (Fig. 7, E–G), the expression level of the *EXS-GFP* gene construct in these lines is significantly different in both shoots and roots (Supplemental Fig. S3). While such variation in expression may result in greater divergence in the overall transcriptomic profile, it is expected that changes in gene expression that are shared between the EXS32 and EXS34 lines are of most significance in understanding the link between EXS expression and shoot growth. Between 22 and 34 million reads were obtained for each tissue/genotype combination and aligned to The Arabidopsis Information Resource (TAIR) 10 genome. Genes with at least a 2-fold change increase (or decrease) compared with *pho1* in any one of the three comparisons (PHO1-C versus *pho1*, EXS32 versus *pho1*, and EXS34 versus *pho1*) were selected and classified with Venn diagrams according to their statistical significance in the three comparisons (false discovery rate [FDR] $< 0.05$; Fig. 9). The largest number of genes showing differential expression was found in shoots. A total of 278 genes were found to be significantly down-regulated in the two EXS-GFP lines compared with the parental *pho1*, and of those, approximately 65% (182 genes) were also down-regulated in *pho1* complemented with PHO1-GFP (Fig. 9A; Supplemental Table S1). Analysis of the 25 most down-regulated genes in leaves of both EXS-GFP lines showed that the majority (greater than 80%) have previously been found in transcriptomic studies to be up-regulated in shoots of Pi-deficient plants (Hammond et al., 2003; Misson et al., 2005; Morcuende et al., 2007; Müller et al., 2007; Woo et al., 2012). They include genes encoding purple acid phosphatases, the SPX-containing proteins SPX1 and SPX3, the RNase RNS1, and the monogalactosyldiacylglycerol synthase MGD3. These results indicate that shoots of *pho1* plants expressing EXS-GFP show an attenuation in the expression of several genes typically up-regulated by Pi deficiency in shoots. Shoots of the two EXS-GFP lines have 95 genes that are commonly up-regulated compared with the parental *pho1* line, with 42 of them being also up-regulated in *pho1* complemented with PHO1-GFP (Fig. 9B; Supplemental Table S2). Analysis of the 25 most up-regulated genes in leaves of both EXS-GFP lines showed that none have been reliably associated with Pi deficiency in previous transcriptomic studies. Interestingly, there is an overrepresentation of genes involved in carbohydrate/cell wall synthesis (16%) or aspects of phytohormone (cytokinin, auxin, and brassinosteroids) synthesis or response (20%).

In comparison with shoots, many fewer genes were differentially expressed in the roots of the EXS-GFP lines. Thus, only 14 genes were commonly down-regulated in roots of the two EXS-GFP lines (Fig. 9C; Supplemental Table S3). Of those, four genes were consistently found in previous transcriptomic studies to be up-regulated under Pi deficiency, namely the *PHO1* homolog *PHO1;H1*, *At1g58340* encoding a multidrug and toxic compound extrusion (MATE) transporter, *At1g01190* encoding a cytochrome P450, and *At1g19960* encoding an unknown protein. Similarly, only eight genes were commonly up-regulated

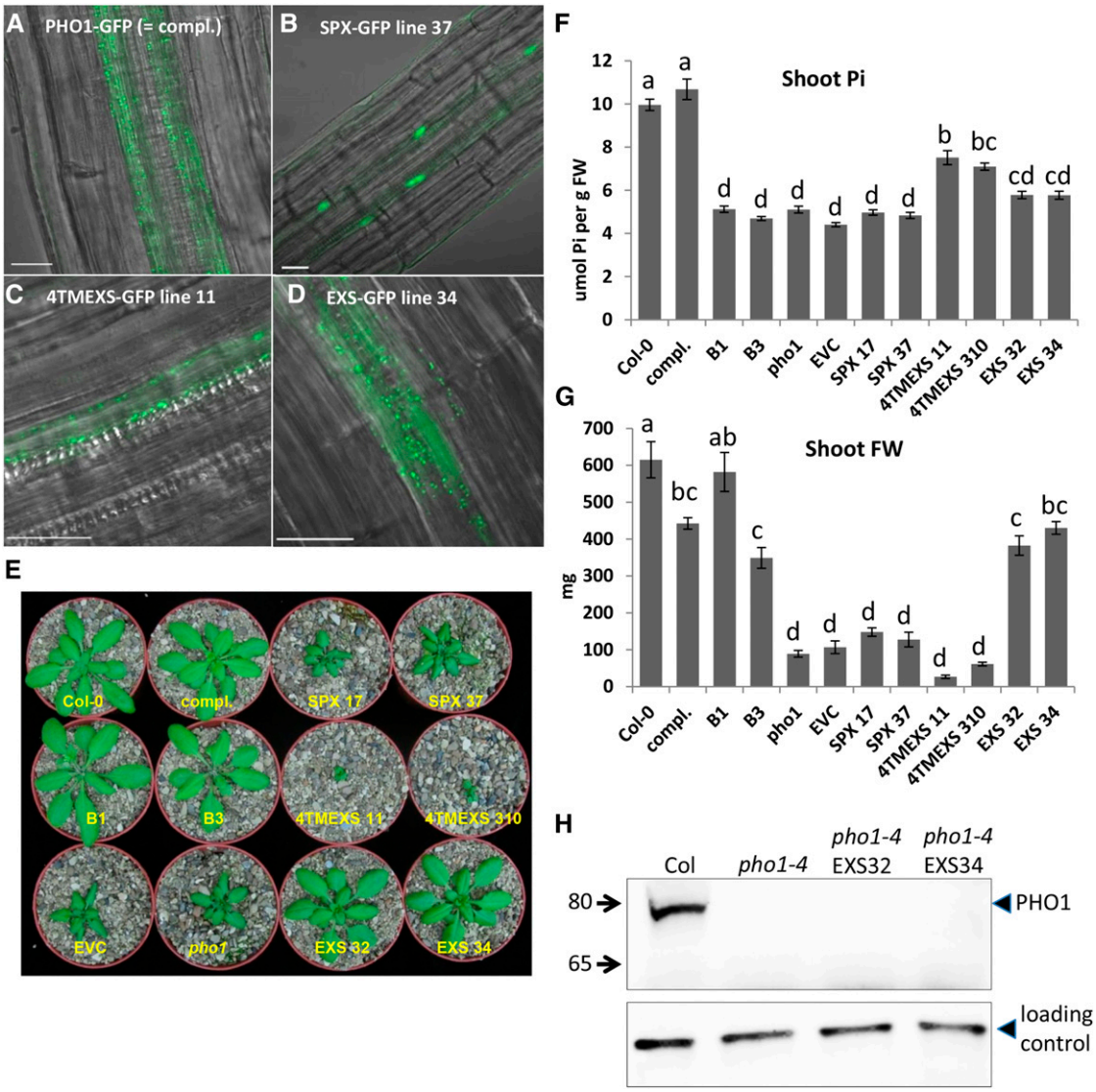


**Figure 7.** Phenotypes of *pho1-4* stably transformed with truncated PHO1-GFP constructs. A to D, Localization of GFP fluorescence from the expression of full-length PHO1-GFP and truncated PHO1-GFP constructs in the root vascular cylinder of *pho1-4* plants. Confocal and transmission light images are superimposed. Bars = 20 $\mu$m. E, Phenotypes of two independent lines of each PHO1 truncation construct transformed in *pho1-4* compared with Columbia-0 (Col-0), *pho1-4*, empty vector control (EVC) in the *pho1-4* background, *pho1-4* complemented with the full-length PHO1-GFP line (compl.), and the two *PHO1* knockdown lines B1 and B3 described previously (Rouached et al., 2011). Plants were grown for 7 d in vitro on plates for confocal imaging and for an additional 25 d in pots for other experiments. F and G, Pi content (F) and fresh weight (FW; G) of the shoots shown in E. Error bars represent SD ($n$ = 10). For all histograms, columns with different letters are significantly different (ANOVA with the Tukey-Kramer test, $P < 0.01$). H, Western-blot analysis of protein extracts of roots from the wild-type Col-0 control, *pho1-4*, and the lines EXS32 and EXS34 expressing EXS-GFP in the *pho1-4* background. Arrows and numbers on the left indicate molecular mass in kD. The bottom gel shows an unspecific band used as a loading control.

in roots of the two EXS-GFP lines, and only the gene encoding a phosphodiesterase (*At5g41080*) was previously associated with Pi deficiency (Fig. 9D; Supplemental Table S4).

A selected set of genes that are responsive to Pi deficiency and/or participate in the Pi signaling response was subsequently analyzed by quantitative reverse transcription (Q-RT)-PCR in shoots of plants expressing SPX-GFP and 4TMEXS-GFP in the *pho1* background. Transgenic lines expressing SPX-GFP showed no or only small differences in the expression of the *IPS1*, *MGD3*, *SPX1*, *PHO1;H1* (the closest homolog to *PHO1*), *PHT1;4*, or *PHO2* genes in the shoots compared with the untransformed *pho1* mutant or *pho1* transformed with an empty vector (Fig. 10). In contrast, the expression of 4TMEXS-GFP in *pho1* resulted in a strong decrease in the expression of *IPS1*, *MGD3*, *SPX1*, and *PHO1;H1* and a weaker decrease in the expression of

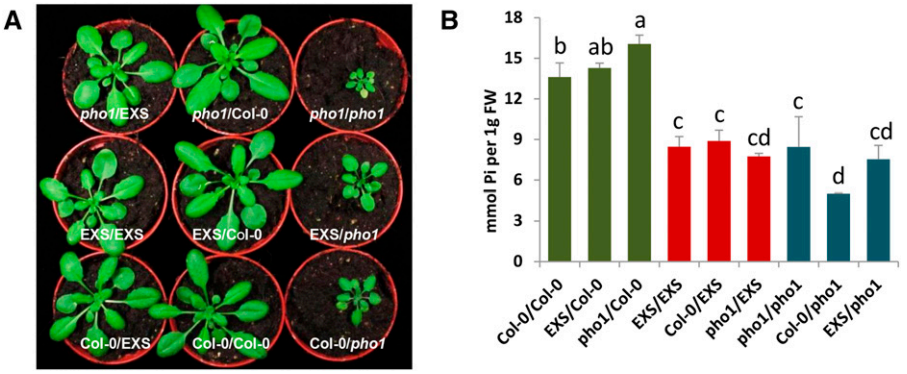


**Figure 8.** Hypocotyl grafts between wild-type Col-0, *pho1-4*, and *pho1-4* plants expressing the EXS domain. For each graft, the numerator and denominator indicate the genotype of the shoot and root, respectively. General appearance (A) and Pi content (B) are shown for shoots of plants grown for 24 d in soil. Error bars represent SD ($n$ = 3–5). For all histograms, columns with different letters are significantly different (ANOVA with the Tukey-Kramer test, $P < 0.01$). FW, Fresh weight.

*PHT1;4*, while *PHO2* expression increased slightly to reach the wild-type level.

## DISCUSSION

Analysis of PHO1 topology using BiFC and roGFP2 revealed that PHO1 has both termini localized toward the cytosol and suggests that the EXS domain contains two transmembrane-spanning segments and a significantly large (approximately 140 amino acids) C-terminal tail. Such an extension could potentially interact with other cytosolic proteins and provide important information on the role of the EXS domain. Apart from PHO1 family members, an EXS domain is found in the yeast ERD1, a protein sharing the topological features of the C-terminal half of PHO1, namely the presence of several transmembrane $\alpha$-helices followed by the EXS domain (Hardwick et al., 1990). Yeast ERD1 was found in proteomic studies to interact with the yeast ER protein retention receptor ERD2 (Miller et al., 2005). Although the function of ERD1 is unknown, its mutation in yeast leads to a defect in Golgi-to-ER protein recycling, suggesting that ERD1 is located in the Golgi and/or ER (Hardwick et al., 1990). ERD1 does not contain other domains apart from EXS. The Arabidopsis genome has two ERD1 homologs, namely At2g32295 and At5g35730, and the latter protein was found in the Golgi in a proteomic study (Parsons et al., 2012).

The EXS domain of PHO1 was found to have several functions. First, it is essential for Pi efflux out of cells. Expression of the SPX4TM truncated protein, lacking the critical EXS domain, does not lead to Pi efflux, either due to its retention in the ER or because the SPX4TM protein is unable to transport Pi. When expressed by itself, the EXS domain of PHO1 was localized at the Golgi/TGN. Together, these data show that the EXS domain of PHO1 contains essential information for the proper localization of PHO1 at the Golgi/TGN, a function that is consistent with the Golgi localization of the EXS-containing protein ERD1 and its plant homologs (Hardwick et al., 1990; Parsons et al., 2012).

Although expression of the EXS domain of PHO1 alone does not mediate Pi export, the expression of EXS in the *pho1* background resulted in a significant improvement of shoot growth despite the maintenance of low shoot Pi content. Such uncoupling between low shoot Pi and robust shoot growth has previously only been found in plants that express low levels of *PHO1* due to gene silencing (Rouached et al., 2010). A grafting experiment performed in our work shows that the expression of EXS in *pho1* roots is sufficient to achieve growth improvement of the Pi-deficient shoot. In the absence of evidence that the *pho1-4* mutant produces any truncated protein that could associate with EXS-GFP, our data support the hypothesis that roots generate a long-distance signal traveling to the shoot to influence growth and that the EXS domain of PHO1 participates in the generation of this long-distance signal.

Improved shoot growth of the *pho1* mutant expressing the EXS domain was associated with reduced expression of a large set of genes typically associated with Pi deficiency in shoots. This included genes encoding enzymes involved in phosphorus scavenging and recycling (e.g. the purple acid phosphatases *PAP5* and *PAP25* and the RNase *RNS1*), lipid modification (the monogalactosyldiacylglycerol synthase *MGD3* and the glycerophosphodiester phosphadiesterase *GDPD6*), and the Pi signaling cascade (*SPX1* and *SPX3*). Such an expression pattern indicates an attenuation of the signal transduction cascade associated with the response to Pi deficiency (Hammond et al., 2003; Misson et al., 2005; Morcuende et al., 2007; Müller et al., 2007; Woo et al., 2012). While the leaf Pi concentration in the EXS lines is similar to the parental *pho1-4*, it is possible that the overall phosphorus status of the EXS plants is improved through changes in the organic phosphorus fraction. Such a change in organic phosphorus may thus influence the expression profile in shoots of the EXS lines. Improved growth was also associated with the increased expression in shoots of a smaller number of genes, with the set of most expressed genes being enriched in genes involved in cell wall biosynthesis (i.e. the glycosyl hydrolase *XYL2*, the $\beta$-xylosidase *BXL3*, the xyloglucan endotransglucosylase *XTH17*, and the

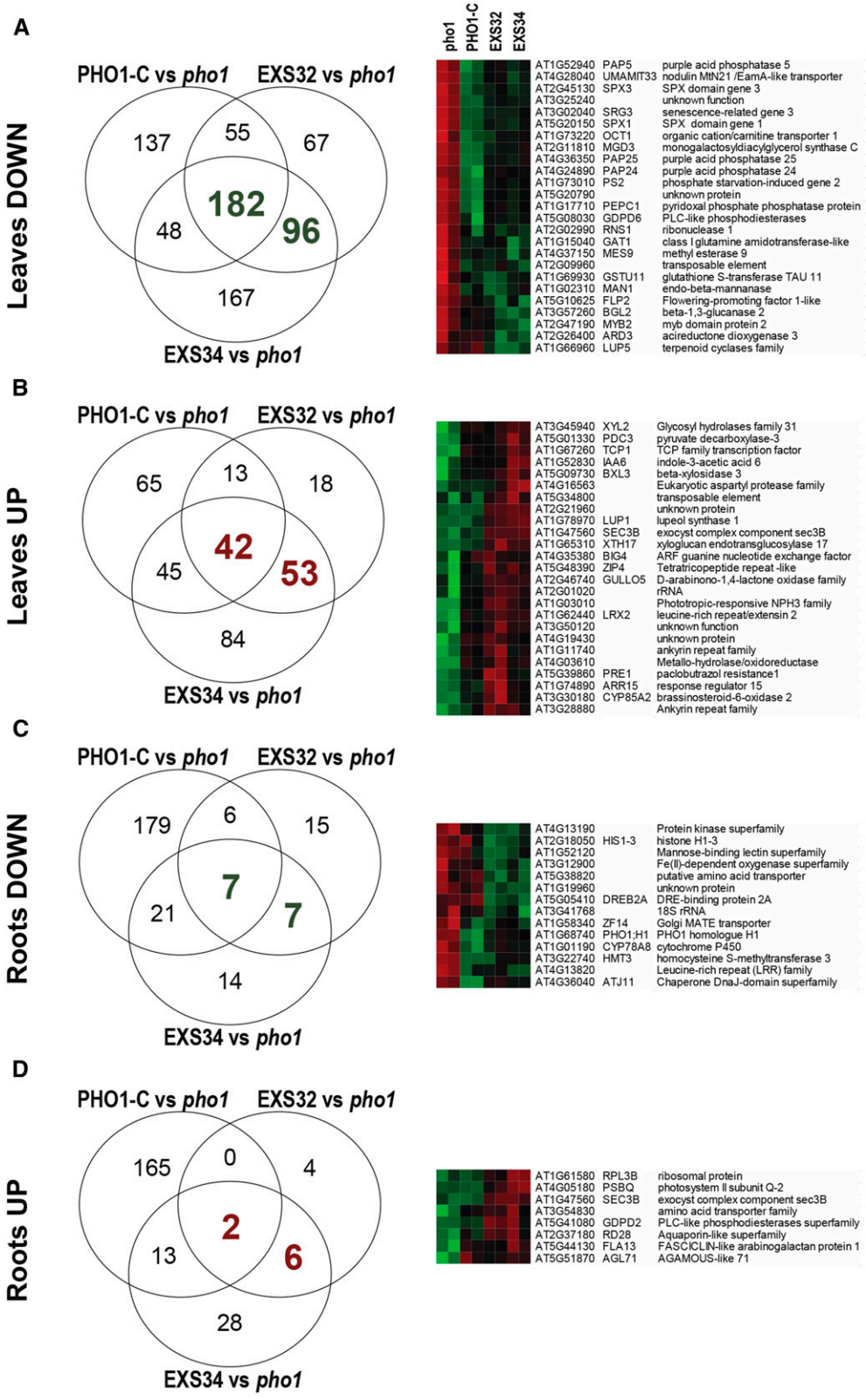


**Figure 9.** Venn diagrams representing the overlap in gene expression profiles in *pho1-4* plants expressing the EXS domain. Gene expression in the roots and leaves of the *pho1-4* mutant was compared with two independent lines of *pho1-4* transformed with the EXS-GFP constructs (lines EXS32 and EXS34) and a *pho1-4* line complemented with the full-length PHO1-GFP construct (PHO1-C). Plants were grown for 25 d in pots, and RNA was extracted from roots and leaves and used for RNAseq analysis. Only genes showing a 2-fold or higher differential expression (FDR $< 0.05$) are shown. Normalized expression values of the genes common to the EXS32 and EXS34 lines are displayed in heat maps. For the leaves, only the 25 most affected genes are shown.

extensin *LRX2*) and phytohormone synthesis or perception, including auxin (the indole-3-acetic acid *IAA6*), cytokinin (the response regulator *ARR15*), and brassinosteroids (brassinosteroid-6-oxidase 2 [*CYP85A2*] and transcription factors TCP1 and PRE1). Interestingly, the majority of these genes have not been associated previously with the Pi deficiency response. They may thus more directly reveal the pathways affected by the EXS

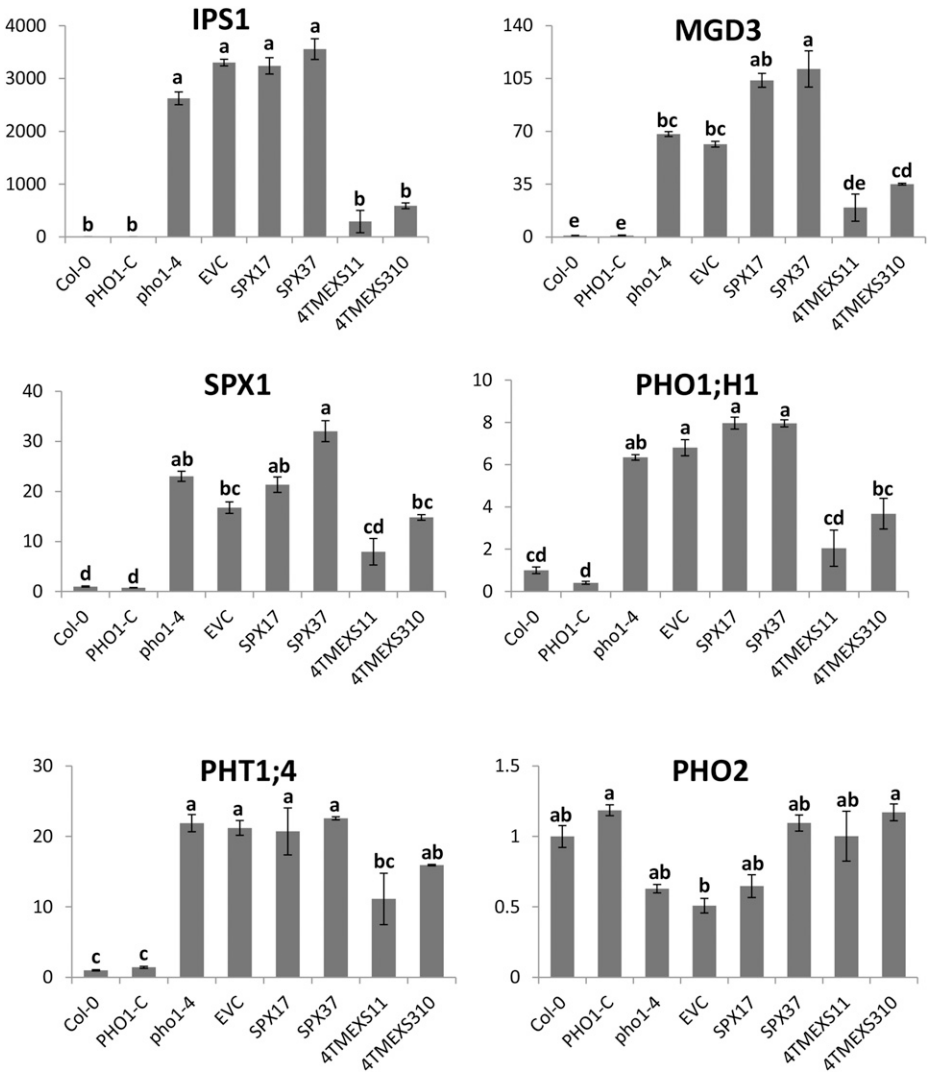


**Figure 10.** Expression of Pi deficiency marker genes in rosettes of *pho1-4* stably transformed with truncated PHO1-GFP constructs. Two independent lines of *pho1-4* transformed with either SPX-GFP or 4TMEXS-GFP were compared with wild-type Col-0, *pho1-4*, *pho1-4* transformed with an empty binary vector (EVC), and *pho1-4* complemented with the full-length PHO1-GFP construct (PHO1-C). Plants were grown for 25 d in pots, RNA was extracted from whole rosettes, and the expression of genes was quantified by Q-RT-PCR. The expression levels are expressed relative to Col-0, which was set at a value of 1. Error bars represent SD ($n = 6$). For all histograms, columns with different letters are significantly different (ANOVA with the Tukey-Kramer test, $P < 0.01$).

domain of PHO1 independently from the Pi status. Cytokinin is known to repress the expression of numerous Pi deficiency-induced genes (Kuiper et al., 1998; Franco-Zorrilla et al., 2002). However, split-root experiments previously argued against a role for cytokinin in the long-distance Pi signaling cascade (Franco-Zorrilla et al., 2005). Auxin and brassinosteroids also influence the architecture of roots in response to Pi deficiency, but neither hormone has been implicated in the Pi deficiency long-distance signaling (Pérez-Torres et al., 2008; Singh et al., 2014). Our results here suggest that the root-to-shoot long-distance signal, influenced by the expression of the EXS domain, may indeed involve the combined action of several phytohormones and that the stimulation of shoot growth may be closely associated with remodeling of the cell wall.

In contrast to shoots, few genes were commonly up- or down-regulated in roots of *pho1* lines expressing EXS relative to the parental *pho1*. It is possible that the expression of the EXS-GFP domain in roots influences shoot growth via changes in proteins or metabolites transported from roots to shoots that are not reflected at the level of the root gene expression profile. Alternatively, it is possible that an alteration of a shoot-to-root signal in the EXS lines leads to changes in root transcript (Lin et al., 2014). Nevertheless, a few interesting observations can be made from inspection of the root transcriptome. A few genes that are down-regulated in the roots of EXS-expressing lines are typically up-regulated by Pi deficiency, such as *PHO1;H1*, encoding the closest homolog of PHO1, as well as *At1G01190* (cytochrome P450), *At1g58340* (Golgi-localized MATE transporter), and *At1g19960* (unknown protein; Hammond et al., 2003; Misson et al., 2005; Morcuende et al., 2007; Müller et al., 2007; Woo et al., 2012). These results may indicate that the suppression of the Pi deficiency response observed in the shoot may also influence the expression of some genes in the roots. Analysis of differentially regulated genes using Genevestigator (www.genevestigator.com) reveals that genes down-regulated in roots by EXS expression are enriched for genes that are down-regulated during seed

germination but up-regulated by treatments implicating abscisic acid (ABA), including salt, heat, cold, or drought stress (*At4g13190*, protein kinase; *At2g18050*, histone H1; *At5g05410*, DREB2A transcription factor; *At3g22740*, homo-Cys-*S*-methyltransferase; and *At4g36040*, chaperone DnaJ family). Conversely, genes up-regulated in roots by EXS expression are enriched for genes that are up-regulated during seed germination and negatively regulated by salt, heat, cold, drought, or ABA treatment (*At2g37180*, aquaporin RD28; *At1g61580*, ribosomal protein RPL3B; *At4g05180*, PSII subunit; and *At5g44130*, fascillin-like arabinogalactan). Although some Pi-responsive genes have been linked previously to ABA and water stress (Woo et al., 2012), the group of genes associated with ABA found in this study are not or are only weakly regulated by Pi deficiency. Together, these results indicate that expression of the EXS domain attenuates the signaling cascades associated with ABA. Such coordination may implicate the DREB2A transcription factor known to control the expression of numerous genes involved in heat and water stress (Sakuma et al., 2006a, 2006b). Of interest is that both *At1g583340*, encoding a MATE efflux protein, and *At5g44130*, encoding a fascillin-like arabinogalactan, are localized to the Golgi and, thus, more directly respond to changes occurring in this compartment by EXS expression (Parsons et al., 2012; Seo et al., 2012).

The SPX domain of PHO1 was not essential for Pi export activity, as the expression of 4TMEXS in *N. benthamiana* leaves mediated Pi export. This is in accordance with the recent finding that the SPX domain of the mammalian PHO1 homolog XPR1 is also not required for Pi export (Giovannini et al., 2013; Wege and Poirier, 2014). However, expression of the SPX-truncated 4TMEXS protein was unable to complement the *pho1* mutant and even strongly exacerbated the reduction in shoot growth. Despite the drastic effect of 4TMEXS expression on shoot growth, expression of the Pi-deficient genes *IPS1*, *MGD3*, *SPX1*, *PHO1;H1*, and *PHT1;4* were all down-regulated. This may be the result of slightly higher shoot Pi content and/or the presence of the EXS domain in the truncated protein. Although the mechanisms implicated in the phenotype of the plants expressing 4TMEXS are unknown, the results suggest an important role for the SPX domain of PHO1 in Arabidopsis. The Arabidopsis genome contains four genes encoding proteins with only an SPX domain, named *AtSPX1* to *AtSPX4* (Wang et al., 2004). Among them, *AtSPX1*, *AtSPX2*, and *AtSPX3* are all strongly up-regulated under Pi deficiency (Duan et al., 2008). AtSPX1 and AtSPX2 proteins are nucleus localized and have recently been shown to bind the PHR1 transcription factor in a Pi-dependent manner, resulting in the disruption of PHR1 binding to its DNA target sequence (Puga et al., 2014). Similar results have also been obtained for the rice OsPHR2 ortholog (Wang et al., 2014). These data suggest that the SPX domain may bind Pi and act as a Pi sensor. It is thus attractive to speculate that the SPX domain of PHO1 may also act as a Pi sensor and modulate either the activity of PHO1 as a Pi exporter in the root stele or as a component of the Pi deficiency signal transduction pathway (Rouached et al., 2011). Transient expression of PHO1 protein domains in *N. benthamiana* leaves is a good system in which to monitor the Pi export function of PHO1; yet, not unexpectedly, it is not suited to reveal more subtle roles in the regulation of PHO1 activity in root cells that may affect more global Pi homeostasis and growth, such as potential interactions with other proteins.

Expression of only the SPX domain of PHO1 led to nuclear localization of the protein in both *N. benthamiana* and Arabidopsis roots, with an additional association with nuclear pores in *N. benthamiana*. Expression of only the SPX domain in the *pho1* mutant did not result in any substantial change in the shoot Pi content, shoot growth, or the level of expression of the Pi-responsive genes in shoot. It is thus unclear at this point if expression of the SPX domain in the nucleus has any biological significance in the context of the mode of action of PHO1 in Pi homeostasis. Generation of nuclear proteins acting on gene transcription from the cleavage of a hydrophilic portion of membrane-bound transporters has been described previously (Gomez-Ospina et al., 2006). However, there is currently no evidence that such a mechanism could apply to PHO1.

Adaptation of plants to Pi deficiency is known to involve both local and long-distance signaling (Chiou and Lin, 2011; Zhang et al., 2014). Local signaling typically affects root system architecture and its response to local Pi supply, such as the reduction of primary root growth by low external Pi at the root tip (López-Bucio et al., 2003; Svistoonoff et al., 2007). In contrast, split-root experiments have shown that long-distance signaling is involved in numerous plant adaptations to Pi deficiency, including the activation of genes involved in Pi uptake, lipid metabolism, and ion transport (Burleigh and Harrison, 1999; Franco-Zorrilla et al., 2005; Thibaud et al., 2010). Shoot-to-root movement of the microRNA mir399 via the phloem was shown to participate in Pi signaling by regulating the ubiquitin-conjugating E2 enzyme PHO2 (Lin et al., 2008; Pant et al., 2008). Yet, components of the root-to-shoot signaling pathway have remained largely elusive but could include proteins, metabolites, hormones, and even RNAs (Thieme et al., 2015). While *pho1* mutants are plants with typical shoot phenotypes associated with Pi deficiency, such as reduced shoot growth, anthocyanin accumulation, and induced expression of numerous Pi deficiency-associated genes, reduced expression of *PHO1* by silencing leads to an uncoupling of Pi deficiency from these effects on shoots (Rouached et al., 2010). This work highlights an important role of the EXS domain of PHO1 in a root-to-shoot signaling pathway linking Pi deficiency with the shoot Pi deficiency syndrome that includes reduced shoot growth. Transcriptome analysis of EXS-expressing *pho1* plants provides a number of new avenues to further explore the Pi deficiency root-to-shoot signaling pathway.

## MATERIALS AND METHODS

### Cloning

Genomic DNA of full-length PHO1 (At3g23430) and PHO1 truncations (amino acids as indicated in Fig. 1B) were first cloned into the Gateway entry vectors pDONR207 or pENTR2B (Invitrogen) and then transferred into the binary plant expression vectors pMDC43, pMDC83, pMDC7, pMDC132, modified p*7WG2, pYFN43, pYFC43, and pSS01 (Karimi et al., 2002; Curtis and Grossniklaus, 2003; Brach et al., 2009; Zimmerli et al., 2012; Wege and Poirier, 2014).

### Plant Growth, Transformation, and Grafting

Arabidopsis (*Arabidopsis thaliana*) and *Nicotiana benthamiana* plants were grown as described previously (Arpat et al., 2012). Arabidopsis Col-0 ecotype was used as the wild type and the *pho1-4* allele as the *pho1* knockout mutant (Hamburger et al., 2002). For transient expression, *N. benthamiana* plants were grown and infiltrated with *Agrobacterium tumefaciens* transformed with binary plasmids as described previously (Arpat et al., 2012). The floral dip method was used for stable Arabidopsis transformation (Clough and Bent, 1998). A modified pMDC132 binary vector, in which the cauliflower mosaic virus 35S promoter was replaced with a 2-kb *PHO1* promoter, was used for the expression of all PHO1 constructs in the *pho1-4* background (Zimmerli et al., 2012). Transformed plant lines were grown 6 d in vitro on one-half-strength Murashige and Skoog medium, 1% (w/v) Suc, and 0.8% (w/v) agar in continuous light, then transferred to pots and grown for 25 d in pots in long-day conditions with 16 h of light at 21°C and 8 h of dark at 20°C. Grafting experiments were performed as described previously (Zimmerli et al., 2012) with the following minor modifications (Marsch-Martínez et al., 2013). Plants for grafts were grown in vitro on one-half-strength Murashige and Skoog medium, 0.5% (w/v) Suc, and 0.8% (w/v) agar for 5 d in short-day conditions with 8 h of light and 16 h of dark at 26°C. During the grafting procedure, silicon tubes were used to strengthen grafts. After grafting, plants were incubated for an additional 5 d on one-half-strength Murashige and Skoog medium and 0.5% (w/v) Suc in short days at 26°C, then transferred to 8 h of light at 21°C and 16 h of dark at 20°C in vitro for an additional 5 d before being transferred to pots and continued to be grown under the same conditions. For RNAseq experiments, plants were grown in Oil Dri US special granulates (http://www.oildri.com/) that were fertilized weekly with a commercial fertilizer (Wuxal; Maag; http://www.maag-garden.ch). Plants were grown in a phytotron with long-day conditions with 16 h of light at 21°C and 8 h of dark at 20°C.

### Western-Blot Analysis

To analyze the PHO1 expression level in roots by western blot, plants were first grown on agar-solidified plates and then shifted to wide-mouth Erlenmeyer flasks containing 15 to 20 mL of one-half-strength Murashige and Skoog liquid medium and 1% (w/v) Suc to produce large amounts of roots from intact plants. Proteins were extracted from homogenized 25-d-old roots at 4°C in extraction buffer containing 10 mM Pi buffer, pH 7.4, 300 mM Suc, 150 mM NaCl, 5 mM EDTA, 5 mM EGTA, 1 mM DTT, 20 mM NaF, and 1× protease inhibitor (Roche EDTA-free complete mini tablet) and sonicated for 10 min in an ice-cold water bath. Fifty micrograms of protein was separated by SDS-PAGE and transferred to an Amersham Hybond-P polyvinylidene difluoride membrane (GE Healthcare). The rabbit polyclonal antibody to PHO1 (Liu et al., 2012) and goat anti-rabbit IgG-horseradish peroxidase (Santa Cruz Biotechnology) were used along with the Western Bright Sirius horseradish peroxidase substrate (Advansta). Signal intensity was measured using a GE Healthcare ImageQuant RT ECL Imager.

### RNAseq Analysis

RNAseq libraries were prepared using 500 ng of total RNA and the Illumina TruSeq Stranded mRNA reagents on a Caliper Sciclone liquid-handling robot (PerkinElmer) using a Caliper-developed automated script. Cluster generation was performed with the resulting libraries using the Illumina TruSeq PE Cluster Kit version 3 reagents and sequenced on the Illumina HiSeq 2500 using TruSeq SBS Kit version 3 reagents. Sequencing data were processed using the Illumina Pipeline Software version 1.82.

Purity-filtered reads were adapters and quality trimmed with Cutadapt (version 1.2.1; Martin, 2011) and filtered for low complexity with Prinseq (version 0.20.3; Schmieder and Edwards, 2011). Reads were aligned against the Arabidopsis genome TAIR 10 using TopHat2 (version 2.0.9; Kim et al., 2013). The number of read counts per gene locus was summarized with htseq-count (version 0.5.4p3; Anders et al., 2015) using TAIR 10 gene annotation. Gene count tables were imported in R (version 3.1.1) for normalization (package edgeR, method TMM; Robinson and Oshlack, 2010) and transformation (package limma, method voom; Law et al., 2014). Leaf and root data were processed separately. Genes with at least one count per million in one sample were kept for further analysis (18,780 in leaves and 19,967 in roots). limma was used to fit a linear model to the expression data with the four conditions as factors (Smyth, 2004). The comparisons PHO1-C versus *pho1*, EXS32 versus *pho1*, and EXS34 versus *pho1* were extracted using contrast matrices. *P* value adjustment for multiple testing with the Benjamini and Hochberg method to control the FDR were performed separately for up- and down-regulated genes after having selected genes with at least a 2-fold change increase (or decrease) in any one of the three comparisons. RNAseq data are deposited at the Gene Expression Omnibus (GSE73067).

### RNA Preparation and Q-RT-PCR

Plant material was immediately frozen in liquid nitrogen. The samples were then ground using a mortar and pestle, and the powder was used to extract the RNA using the RNeasy Plant Mini Kit (Qiagen). Samples were treated with DNase on columns during RNA extraction using the RNase-free DNase kit (Qiagen). For gene expression by Q-RT-PCR, 500 ng of RNA per sample was used for reverse transcription using SuperScript II reverse transcriptase (Invitrogen). Q-RT-PCR was performed using SYBER Select Master Mix (Invitrogen) and the Stratagene Mx3005p qPCR system.

### Pi and Nitrate Export

For the determination of Pi and nitrate content in plant tissues, the cellular content of cells was first released into distilled water by repeated freeze/thaw cycles followed by incubation at 80°C for 30 min. Pi concentration in the solution was then quantified by the molybdate assay (Ames, 1966). Nitrate was quantified by first converting nitrate to nitrite using commercial nitrate reductase from *Aspergillus niger* (Sigma) followed by nitrite quantification using sulfanilamide as described previously (Barthes et al., 1995).

### Confocal Microscopy

Subcellular localization of GFP and RFP fusion constructs and BiFC experiments in Arabidopsis roots and *N. benthamiana* leaf epidermal cells were performed using a Zeiss LSM 700 confocal microscope with an Apochromat 63× water-immersion differential interference contrast objective with a numerical aperture of 1.2. Analysis of roGFP2 was performed using a Zeiss LSM780 confocal microscope with a 40× 1.2 numerical aperture C-Apochromat water-immersion lens. Images were collected in multitrack mode with line switching between 488 and 405 nm illumination.

The roGFP fluorescence was collected in the 505- to 530-nm emission band, and data analysis was done as described previously (Brach et al., 2009).

### Supplemental Data

The following supplemental materials are available.

**Supplemental Figure S1.** Prediction of PHO1 topology as obtained from ARAMEMNON

**Supplemental Figure S2.** Investigation of PHO1 topology using BiFC in *N. benthamiana*.

**Supplemental Figure S3.** Expression of the EXS-GFP construct in the EXS32 and EXS34 lines.

**Supplemental Table S1.** List of genes with a significant decrease (FDR < 0.05) and 2-fold or higher change in leaves compared with *pho1-4* in any one of the three comparisons.

**Supplemental Table S2.** List of genes with a significant increase (FDR < 0.05) and 2-fold or higher change in leaves compared with *pho1-4* in any one of the three comparisons.

**Supplemental Table S3.** List of genes with a significant decrease (FDR < 0.05) and 2-fold or higher change in roots compared with *pho1-4* in any one of the three comparisons.

**Supplemental Table S4.** List of genes with a significant increase (FDR < 0.05) and 2-fold or higher change in roots compared with *pho1-4* in any one of the three comparisons.

## ACKNOWLEDGMENTS

We thank David L. Spector (Cold Spring Harbor Laboratory) for helpful suggestions on nuclear pores, Tzyy-Jen Chiou (Academia Sinica) for antibodies against PHO1, and the University of Lausanne Genomic Technologies Facility for high-throughput sequencing support.

Received June 30, 2015; accepted November 4, 2015; published November 6, 2015.

## LITERATURE CITED

**Ames BN** (1966) Assay of inorganic phosphate, total phosphate and phosphatases. Methods Enzymol **8:** 115–118

**Anders S, Pyl PT, Huber W** (2015) HTSeq: a Python framework to work with high-throughput sequencing data. Bioinformatics **31:** 166–169

**Arpat AB, Magliano P, Wege S, Rouached H, Stefanovic A, Poirier Y** (2012) Functional expression of PHO1 to the Golgi and *trans*-Golgi network and its role in export of inorganic phosphate. Plant J **71:** 479–491

**Barberon M, Zelazny E, Robert S, Conéjéro G, Curie C, Friml J, Vert G** (2011) Monoubiquitin-dependent endocytosis of the iron-regulated transporter 1 (IRT1) transporter controls iron uptake in plants. Proc Natl Acad Sci USA **108:** E450–E458

**Barthes L, Bousser A, Hoarau J, Deleens E** (1995) Reassessment of the relationship between nitrogen supply and xylem exudation in detopped maize seedlings. Plant Physiol Biochem **33:** 173–183

**Battini JL, Rasko JEJ, Miller AD** (1999) A human cell-surface receptor for xenotropic and polytropic murine leukemia viruses: possible role in G protein-coupled signal transduction. Proc Natl Acad Sci USA **96:** 1385–1390

**Bernsel A, Viklund H, Hennerdal A, Elofsson A** (2009) TOPCONS: consensus prediction of membrane protein topology. Nucleic Acids Res **37:** W465–W468

**Bonfante P, Genre A** (2010) Mechanisms underlying beneficial plant-fungus interactions in mycorrhizal symbiosis. Nat Commun **1:** 48

**Brach T, Soyk S, Müller C, Hinz G, Hell R, Brandizzi F, Meyer AJ** (2009) Non-invasive topology analysis of membrane proteins in the secretory pathway. Plant J **57:** 534–541

**Burleigh SH, Harrison MJ** (1999) The down-regulation of *Mt4*-like genes by phosphate fertilization occurs systemically and involves phosphate translocation to the shoots. Plant Physiol **119:** 241–248

**Chiou TJ, Lin SI** (2011) Signaling network in sensing phosphate availability in plants. Annu Rev Plant Biol **62:** 185–206

**Clough SJ, Bent AF** (1998) Floral dip: a simplified method for *Agrobacterium*-mediated transformation of *Arabidopsis thaliana*. Plant J **16:** 735–743

**Curtis MD, Grossniklaus U** (2003) A Gateway cloning vector set for high-throughput functional analysis of genes in planta. Plant Physiol **133:** 462–469

**Duan K, Yi K, Dang L, Huang H, Wu W, Wu P** (2008) Characterization of a sub-family of Arabidopsis genes with the SPX domain reveals their diverse functions in plant tolerance to phosphorus starvation. Plant J **54:** 965–975

**Franco-Zorrilla JM, Martín AC, Leyva A, Paz-Ares J** (2005) Interaction between phosphate-starvation, sugar, and cytokinin signaling in Arabidopsis and the roles of cytokinin receptors CRE1/AHK4 and AHK3. Plant Physiol **138:** 847–857

**Franco-Zorrilla JM, Martin AC, Solano R, Rubio V, Leyva A, Paz-Ares J** (2002) Mutations at *CRE1* impair cytokinin-induced repression of phosphate starvation responses in Arabidopsis. Plant J **32:** 353–360

**Giovannini D, Touhami J, Charnet P, Sitbon M, Battini JL** (2013) Inorganic phosphate export by the retrovirus receptor XPR1 in metazoans. Cell Reports **3:** 1866–1873

**Gomez-Ospina N, Tsuruta F, Barreto-Chang O, Hu L, Dolmetsch R** (2006) The C terminus of the L-type voltage-gated calcium channel Ca(V)1.2 encodes a transcription factor. Cell **127:** 591–606

**Hamburger D, Rezzonico E, MacDonald-Comber Petétot J, Somerville C, Poirier Y** (2002) Identification and characterization of the *Arabidopsis PHO1* gene involved in phosphate loading to the xylem. Plant Cell **14:** 889–902

**Hammond JP, Bennett MJ, Bowen HC, Broadley MR, Eastwood DC, May ST, Rahn C, Swarup R, Woolaway KE, White PJ** (2003) Changes in gene expression in Arabidopsis shoots during phosphate starvation and the potential for developing smart plants. Plant Physiol **132:** 578–596

**Hardwick KG, Lewis MJ, Semenza J, Dean N, Pelham HR** (1990) *ERD1*, a yeast gene required for the retention of luminal endoplasmic reticulum proteins, affects glycoprotein processing in the Golgi apparatus. EMBO J **9:** 623–630

**He L, Zhao M, Wang Y, Gai J, He C** (2013) Phylogeny, structural evolution and functional diversification of the plant PHOSPHATE1 gene family: a focus on Glycine max. BMC Evol Biol **13:** 103

**Hothorn M, Neumann H, Lenherr ED, Wehner M, Rybin V, Hassa PO, Uttenweiler A, Reinhardt M, Schmidt A, Seiler J, et al** (2009) Catalytic core of a membrane-associated eukaryotic polyphosphate polymerase. Science **324:** 513–516

**Kant S, Peng M, Rothstein SJ** (2011) Genetic regulation by NLA and microRNA827 for maintaining nitrate-dependent phosphate homeostasis in Arabidopsis. PLoS Genet **7:** e1002021

**Karimi M, Inzé D, Depicker A** (2002) GATEWAY vectors for Agrobacterium-mediated plant transformation. Trends Plant Sci **7:** 193–195

**Kim D, Pertea G, Trapnell C, Pimentel H, Kelley R, Salzberg SL** (2013) TopHat2: accurate alignment of transcriptomes in the presence of insertions, deletions and gene fusions. Genome Biol **14:** R36

**Kriechbaumer V, Wang P, Hawes C, Abell BM** (2012) Alternative splicing of the auxin biosynthesis gene YUCCA4 determines its subcellular compartmentation. Plant J **70:** 292–302

**Kuiper D, Schuit J, Kuiper PJC** (1998) Effect of internal and external cytokinin concentrations on root growth and shoot to root ratio of *Plantago major* ssp. *pleiosperma* at different nutrient concentrations. Plant Soil **111:** 231–236

**Law CW, Chen Y, Shi W, Smyth GK** (2014) voom: precision weights unlock linear model analysis tools for RNA-seq read counts. Genome Biol **15:** R29

**Lin SI, Chiang SF, Lin WY, Chen JW, Tseng CY, Wu PC, Chiou TJ** (2008) Regulatory network of microRNA399 and PHO2 by systemic signaling. Plant Physiol **147:** 732–746

**Lin WY, Huang TK, Chiou TJ** (2013) Nitrogen limitation adaptation, a target of microRNA827, mediates degradation of plasma membrane-localized phosphate transporters to maintain phosphate homeostasis in *Arabidopsis*. Plant Cell **25:** 4061–4074

**Lin WY, Huang TK, Leong SJ, Chiou TJ** (2014) Long-distance call from phosphate: systemic regulation of phosphate starvation responses. J Exp Bot **65:** 1817–1827

**Liu TY, Huang TK, Tseng CY, Lai YS, Lin SI, Lin WY, Chen JW, Chiou TJ** (2012) PHO2-dependent degradation of PHO1 modulates phosphate homeostasis in *Arabidopsis*. Plant Cell **24:** 2168–2183

**López-Bucio J, Cruz-Ramírez A, Herrera-Estrella L** (2003) The role of nutrient availability in regulating root architecture. Curr Opin Plant Biol **6:** 280–287

**Lv Q, Zhong Y, Wang Y, Wang Z, Zhang L, Shi J, Wu Z, Liu Y, Mao C, Yi K, et al** (2014) SPX4 negatively regulates phosphate signaling and homeostasis through its interaction with PHR2 in rice. Plant Cell **26:** 1586–1597

**Marsch-Martínez N, Franken J, Gonzalez-Aguilera KL, de Folter S, Angenent G, Alvarez-Buylla ER** (2013) An efficient flat-surface collar-free grafting method for *Arabidopsis thaliana* seedlings. Plant Methods **9:** 14

**Martin M** (2011) Cutadapt removes adapter sequences from high-throughput sequencing reads. EMBnet J **17:** 10–12

**Miller JP, Lo RS, Ben-Hur A, Desmarais C, Stagljar I, Noble WS, Fields S** (2005) Large-scale identification of yeast integral membrane protein interactions. Proc Natl Acad Sci USA **102:** 12123–12128

**Misson J, Raghothama KG, Jain A, Jouhet J, Block MA, Bligny R, Ortet P, Creff A, Somerville S, Rolland N, et al** (2005) A genome-wide transcriptional analysis using *Arabidopsis thaliana* Affymetrix gene chips determined plant responses to phosphate deprivation. Proc Natl Acad Sci USA **102:** 11934–11939

**Morcuende R, Bari R, Gibon Y, Zheng W, Pant BD, Bläsing O, Usadel B, Czechowski T, Udvardi MK, Stitt M, et al** (2007) Genome-wide

reprogramming of metabolism and regulatory networks of Arabidopsis in response to phosphorus. Plant Cell Environ **30:** 85–112

**Müller R, Morant M, Jarmer H, Nilsson L, Nielsen TH** (2007) Genome-wide analysis of the Arabidopsis leaf transcriptome reveals interaction of phosphate and sugar metabolism. Plant Physiol **143:** 156–171

**Nelson BK, Cai X, Nebenführ A** (2007) A multicolored set of in vivo organelle markers for co-localization studies in Arabidopsis and other plants. Plant J **51:** 1126–1136

**Pant BD, Buhtz A, Kehr J, Scheible WR** (2008) MicroRNA399 is a long-distance signal for the regulation of plant phosphate homeostasis. Plant J **53:** 731–738

**Parsons HT, Christiansen K, Knierim B, Carroll A, Ito J, Batth TS, Smith-Moritz AM, Morrison S, McInerney P, Hadi MZ, et al** (2012) Isolation and proteomic characterization of the Arabidopsis Golgi defines functional and novel components involved in plant cell wall biosynthesis. Plant Physiol **159:** 12–26

**Pérez-Torres CA, López-Bucio J, Cruz-Ramírez A, Ibarra-Laclette E, Dharmasiri S, Estelle M, Herrera-Estrella L** (2008) Phosphate availability alters lateral root development in *Arabidopsis* by modulating auxin sensitivity via a mechanism involving the TIR1 auxin receptor. Plant Cell **20:** 3258–3272

**Poirier Y, Bucher M** (2002) Phosphate transport and homeostasis in Arabidopsis. The Arabidopsis Book **1:** e0024, doi/10.1199/tab.0024

**Poirier Y, Thoma S, Somerville C, Schiefelbein J** (1991) Mutant of Arabidopsis deficient in xylem loading of phosphate. Plant Physiol **97:** 1087–1093

**Puga MI, Mateos I, Charukesi R, Wang Z, Franco-Zorrilla JM, de Lorenzo L, Irigoyen ML, Masiero S, Bustos R, Rodríguez J, et al** (2014) SPX1 is a phosphate-dependent inhibitor of Phosphate Starvation Response 1 in Arabidopsis. Proc Natl Acad Sci USA **111:** 14947–14952

**Robinson MD, Oshlack A** (2010) A scaling normalization method for differential expression analysis of RNA-seq data. Genome Biol **11:** R25

**Rouached H, Arpat AB, Poirier Y** (2010) Regulation of phosphate starvation responses in plants: signaling players and cross-talks. Mol Plant **3:** 288–299

**Rouached H, Stefanovic A, Secco D, Bulak Arpat A, Gout E, Bligny R, Poirier Y** (2011) Uncoupling phosphate deficiency from its major effects on growth and transcriptome via PHO1 expression in Arabidopsis. Plant J **65:** 557–570

**Sakuma Y, Maruyama K, Osakabe Y, Qin F, Seki M, Shinozaki K, Yamaguchi-Shinozaki K** (2006a) Functional analysis of an *Arabidopsis* transcription factor, DREB2A, involved in drought-responsive gene expression. Plant Cell **18:** 1292–1309

**Sakuma Y, Maruyama K, Qin F, Osakabe Y, Shinozaki K, Yamaguchi-Shinozaki K** (2006b) Dual function of an Arabidopsis transcription factor DREB2A in water-stress-responsive and heat-stress-responsive gene expression. Proc Natl Acad Sci USA **103:** 18822–18827

**Schmieder R, Edwards R** (2011) Quality control and preprocessing of metagenomic datasets. Bioinformatics **27:** 863–864

**Schwacke R, Schneider A, van der Graaff E, Fischer K, Catoni E, Desimone M, Frommer WB, Flügge UI, Kunze R** (2003) ARAMEMNON, a novel database for Arabidopsis integral membrane proteins. Plant Physiol **131:** 16–26

**Secco D, Baumann A, Poirier Y** (2010) Characterization of the rice PHO1 gene family reveals a key role for OsPHO1;2 in phosphate homeostasis and the evolution of a distinct clade in dicotyledons. Plant Physiol **152:** 1693–1704

**Secco D, Wang C, Arpat BA, Wang Z, Poirier Y, Tyerman SD, Wu P, Shou H, Whelan J** (2012) The emerging importance of the SPX domain-containing proteins in phosphate homeostasis. New Phytol **193:** 842–851

**Seo PJ, Park J, Park MJ, Kim YS, Kim SG, Jung JH, Park CM** (2012) A Golgi-localized MATE transporter mediates iron homoeostasis under osmotic stress in Arabidopsis. Biochem J **442:** 551–561

**Singh A, Fridman Y, Friedlander-Shami L, Tarkowska D, Strnad M, Savaldi-Goldstein S** (2014) Activity of the brassinosteroid transcription factors BRASSINAZOLE RESISTANT1 and BRASSINOSTEROID INSENSITIVE1-ETHYL METHANESULFONATE-SUPPRESSOR1/BRASSINAZOLE RESISTANT2 blocks developmental reprogramming in response to low phosphate availability. Plant Physiol **166:** 678–688

**Smyth GK** (2004) Linear models and empirical Bayes methods for assessing differential expression in microarray experiments. Stat Appl Genet Mol Biol **3:** e3

**Sparkes I, Tolley N, Aller I, Svozil J, Osterrieder A, Botchway S, Mueller C, Frigerio L, Hawes C** (2010) Five *Arabidopsis* reticulon isoforms share endoplasmic reticulum location, topology, and membrane-shaping properties. Plant Cell **22:** 1333–1343

**Stadler R, Lauterbach C, Sauer N** (2005) Cell-to-cell movement of green fluorescent protein reveals post-phloem transport in the outer integument and identifies symplastic domains in Arabidopsis seeds and embryos. Plant Physiol **139:** 701–712

**Suntharalingam M, Wente SR** (2003) Peering through the pore: nuclear pore complex structure, assembly, and function. Dev Cell **4:** 775–789

**Svistoonoff S, Creff A, Reymond M, Sigoillot-Claude C, Ricaud L, Blanchet A, Nussaume L, Desnos T** (2007) Root tip contact with low-phosphate media reprograms plant root architecture. Nat Genet **39:** 792–796

**Thibaud MC, Arrighi JF, Bayle V, Chiarenza S, Creff A, Bustos R, Paz-Ares J, Poirier Y, Nussaume L** (2010) Dissection of local and systemic transcriptional responses to phosphate starvation in Arabidopsis. Plant J **64:** 775–789

**Thieme C, Rojas-Triana M, Stecyk E, Schudoma C, Zhang W, Yang L, Miñambres M, Walther D, Schulze W, Paz-Ares J, et al** (2015) Endogenous Arabidopsis messenger RNAs transported to distant tissues. Nature Plants **1:** e15025

**Wang P, Hummel E, Osterrieder A, Meyer AJ, Frigerio L, Sparkes I, Hawes C** (2011) KMS1 and KMS2, two plant endoplasmic reticulum proteins involved in the early secretory pathway. Plant J **66:** 613–628

**Wang Y, Ribot C, Rezzonico E, Poirier Y** (2004) Structure and expression profile of the Arabidopsis *PHO1* gene family indicates a broad role in inorganic phosphate homeostasis. Plant Physiol **135:** 400–411

**Wang Y, Secco D, Poirier Y** (2008) Characterization of the *PHO1* gene family and the responses to phosphate deficiency of *Physcomitrella patens*. Plant Physiol **146:** 646–656

**Wang Z, Ruan W, Shi J, Zhang L, Xiang D, Yang C, Li C, Wu Z, Liu Y, Yu Y, et al** (2014) Rice SPX1 and SPX2 inhibit phosphate starvation responses through interacting with PHR2 in a phosphate-dependent manner. Proc Natl Acad Sci USA **111:** 14953–14958

**Wege S, Poirier Y** (2014) Expression of the mammalian Xenotropic Polytropic Virus Receptor 1 (XPR1) in tobacco leaves leads to phosphate export. FEBS Lett **588:** 482–489

**Woo J, MacPherson CR, Liu J, Wang H, Kiba T, Hannah MA, Wang XJ, Bajic VB, Chua NH** (2012) The response and recovery of the Arabidopsis thaliana transcriptome to phosphate starvation. BMC Plant Biol **12:** 62

**Wykoff DD, O'Shea EK** (2001) Phosphate transport and sensing in *Saccharomyces cerevisiae*. Genetics **159:** 1491–1499

**Yang YL, Guo L, Xu S, Holland CA, Kitamura T, Hunter K, Cunningham JM** (1999) Receptors for polytropic and xenotropic mouse leukaemia viruses encoded by a single gene at Rmc1. Nat Genet **21:** 216–219

**Zamyatnin AA Jr, Solovyev AG, Bozhkov PV, Valkonen JPT, Morozov SY, Savenkov EI** (2006) Assessment of the integral membrane protein topology in living cells. Plant J **46:** 145–154

**Zhang Z, Liao H, Lucas WJ** (2014) Molecular mechanisms underlying phosphate sensing, signaling, and adaptation in plants. J Integr Plant Biol **56:** 192–220

**Zimmerli C, Ribot C, Vavasseur A, Bauer H, Hedrich R, Poirier Y** (2012) PHO1 expression in guard cells mediates the stomatal response to abscisic acid in Arabidopsis. Plant J **72:** 199–211